3D Direct Laser Writing of Highly Absorptive Photoresist for Miniature Optical Apertures

Michael D. Schmid,* Andrea Toulouse, Simon Thiele, Simon Mangold, Alois M. Herkommer, and Harald Giessen

The importance of 3D direct laser writing as an enabling technology increased rapidly in recent years. Complex micro-optics and optical devices with various functionalities are now feasible. Different possibilities to increase the optical performance are demonstrated, for example, multi-lens objectives, a combination of different photoresists, or diffractive optical elements. It is still challenging to create fitting apertures for these micro optics. In this work, a novel and simple way to create 3D-printed opaque structures with a highly absorptive photoresist is introduced, which can be used to fabricate microscopic apertures increasing the contrast of 3D-printed micro optics and enabling new optical designs. Both hybrid printing by combining clear and opaque resists, as well as printing transparent optical elements and their surrounding opaque apertures solely from a single black resist by using different printing thicknesses are demonstrated.

1. Introduction

The use of 3D direct laser writing as a fast and highly accurate fabrication process for nano- and micro-optical devices is widely used in different scientific fields such as biology,[1–3] microfluidics,[4–8] imaging,[9,10] optical communication,[11–13] beam

M. D. Schmid, S. Mangold, H. Giessen
4th Physics Institute
University of Stuttgart
Pfaffenwaldring 57, 70569 Stuttgart, Germany
E-mail: m.schmid@pi4.uni-stuttgart.de

M. D. Schmid, A. Toulouse, S. Thiele, S. Mangold, A. M. Herkommer, H. Giessen
Research Center SCoPE
University of Stuttgart
Pfaffenwaldring 57, 70569 Stuttgart, Germany

A. Toulouse, S. Thiele, A. M. Herkommer
Institute of Applied Optics (ITO)
University of Stuttgart
Pfaffenwaldring 9, 70569 Stuttgart, Germany

S. Thiele
Printoptix GmbH
Johannesstraße 11, 70176 Stuttgart, Germany

The ORCID identification number(s) for the author(s) of this article can be found under https://doi.org/10.1002/adfm.202211159.

shaping,[14–17] sensing,[18–25] trapping,[26,27] or endoscopy.[28–31] Furthermore, the complexity of 3D-printed optics increased drastically over the years by utilizing new optical designs with multi-lens objectives,[32–35] diffractive surfaces,[36] novel photoresists with different dispersion and their combination,[37,38] or even moving parts.[39] Novel material classes such as glass ceramics[40] or hybrid organic-inorganic polymer resists[41] further broaden possible applications. For optical performance, apertures play a crucial role as a fundamental design component. However, they could not be 3D printed to date. There are other fabrication methods to include apertures in 3D printed micro optics, but they include additional fabrication steps and tools such as filling 3D printed voids with black ink or evaporation of opaque materials.[32,42] In this work we demonstrate for the first time how the black photoresist Prototype IP-Black (Nanoscribe GmbH & Co. KG) can be polymerized via 3D direct laser writing and thus can be utilized to fabricate arbitrary complex micro-apertures, enabling new optical designs. We characterize the photoresist in terms of absorption as well as dispersion and use this knowledge of the material parameters to create different 3D direct laser-written apertures in combination with different lens designs consisting of standard photoresists such as IP-S (Nanoscribe GmbH & Co. KG). Since there is enough light transmitted through flat singlet lenses we demonstrate that it is even possible to create a lens and aperture in a single step with the highly absorptive photoresist, drastically reducing the fabrication complexity and time.

2. Material Properties

Prototype IP-Black is a one-component cationically curing epoxy-resin system. The material is solely light-curing with an added photoinitiator in the ultraviolet (UV), making it suitable for direct laser writing. The viscosity of the material is 300 mPas. This is relatively low compared to other typically used photoresists for 3D direct laser writing. However, it can still be used for two-photon polymerization (2PP) lithography. For the user, no special preparation or treatment of the resist is necessary. To characterize the transmission of the black photoresist we print patches with a side length of 250 µm with
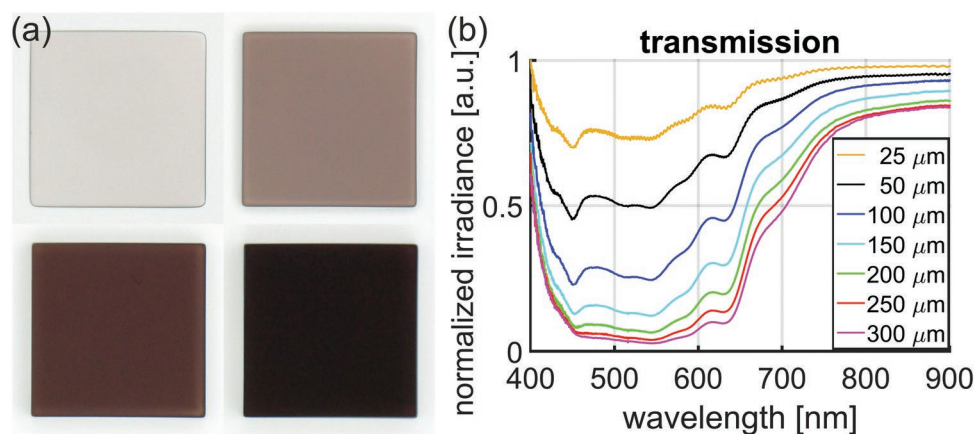
Figure 1. a) Through illumination images of squares made of the black photoresist with different thicknesses of 50, 100, 150, and 200 µm. b) Transmission spectra in the visible for squares made of the black photoresist with thickness ranging from 25 µm to 300 µm. The transmission decreases with increased thickness. The photoresist shows the strongest absorption in the visible between 450 and 650 nm.

different heights from 25 µm to 300 µm (**Figure 1**a). We use a Nanoscribe Photonic Professional GT direct laser writing machine on indium tin oxide-coated glass substrates. For the fabrication of the different apertures, we use the wrapped femtosecond direct laser writing method[43] to avoid any contact of the material with the objective and possible coloring. We use the wrapped objective in dip-in mode resulting in a constant beam path length through the material thus constant writing intensity in the focal spot. This also enables structure heights exceeding the working distance of the objective. The writing parameters are: Slicing 2 µm, hatching 1 µm, laser power 100% (≈58 mW, with a repetition rate of 80 MHz, the pulse energy is 725 pJ or intensity of 3.7 TW cm^{-2}), scan speed 40 mm s^{-1}. Due to an extinction coefficient of ≈1 per mm at 780 nm the laser power reduces to ≈70% in the focal spot or intensity of 2.6 TW cm^{-2}. We use a 25× Zeiss objective (LCI "Plan-Neofluar" 25×/0.8) with a working distance of 380 µm. After the printing process, the sample is developed in mr-Dev 600 for 15 min to remove residual photoresist and afterward cleaned in isopropanol for 5 min. For the transmission measurement, we use an inverted microscope (Nikon Eclipse TE2000-U) attached to a Princeton Instruments Acton Advanced SP 2500i grating spectrometer, equipped with a Pixis-256e Peltier-cooled CCD camera. We illuminate the sample with a fiber-coupled halogen lamp (Oriel) using critical illumination under a maximum numerical aperture (NA) of 0.65. The transmitted light is projected onto the entrance slit of the spectrometer using a Nikon TU Plan Fluor ELWD 60X objective (NA 0.70). In order to normalize the measurements, we used the spectrum of a resist-free area on the same indium tin oxide-coated substrate as a reference. The resulting transmittance is depicted in Figure 1b. As expected, the transmission reduces with increased photoresist layer thickness. For the patch with a height of 25 µm the lowest transmitted intensity is still ≈75%. With a height of 250 µm, the transmitted intensity between 450 and 650 nm is below 5%, but at wavelengths below 450 nm and above 650 nm it is much higher. The absorption is mainly in the visible, which is beneficial for the 3D direct laser writing fabrication process since the laser beam at 780 nm can pass through the photoresist without too much intensity reduction and can still polymerize

the photoresist in the focal spot. Using these results, apertures with a thickness of above 250 µm should exhibit good performance and can be fabricated via 3D direct laser writing.

Another important material parameter is the refractive index and dispersion of the material. For the measurement, we use a commercially available refractometer SCHMIDT + HAENSCH ATR-L and measure the dispersion between 400 nm and 900 nm for the liquid photoresist, and after UV treatment with a UV lamp (15, 30, and 45 min UV exposure with a DymaxBlue-Wave 50 delivering UV light at 365 nm with an intensity of 3000 mW cm^{-2}, at a distance of 3 cm with a resulting intensity of 250 mW cm^{-2}, photoresist layer thickness ≈1 mm) presented in **Figure 2**. The photoresist can be polymerized with the UV lamp due to the low absorption in this wavelength region. The refractive indices of the liquid photoresist
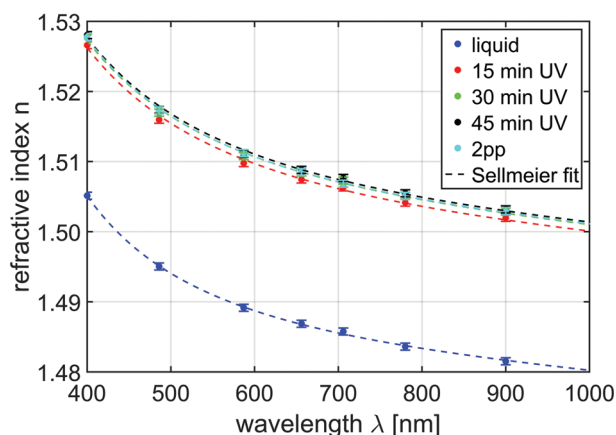

Figure 2. Refractive index measurement of the Prototype IP-Black photoresist in the visible from 400 nm to 900 nm for different UV illumination times. The liquid photoresist has refractive indices between 1.505 and 1.48. During UV treatment and the resulting polymerization the refractive index increases, depending on the dose. After 30 min of illumination, the refractive index has reached a saturation point at ≈0.02 above the liquid photoresist. A 3D direct laser written test patch of 5 mm diameter and 250 µm height exhibits similar refractive indices. We used a fine slicing of 0.2 µm and hatching of 0.5 µm to match the fabrication parameters of the later presented micro-optics.

**ADVANCED
SCIENCE NEWS**

www.advancedsciencenews.com

**ADVANCED
FUNCTIONAL
MATERIALS**

www.afm-journal.de

range from 1.48 to 1.505. After 15 min UV exposure the refractive indices increase and saturate for longer exposure times after 30 min in a range from 1.50 to 1.528. A 3D direct laser written patch of 5 mm diameter and 250 µm height was created (same writing parameters as the patches but finer slicing of 0.2 µm and hatching of 0.5 µm equal to the later presented micro-optics), exhibiting very similar refractive indices. This indicates that after the long UV curing or direct laser writing with high intensity the polymerization of the material saturates. The Abbe number of the 2PP photoresist is 55 and the refractive indices are very close to the commonly used 3D direct laser writing photoresist IP-S from NanoScribe GmbH.[44] The Sellmeier fit $n(\lambda)^2 = 1 + \frac{B_1\lambda^2}{\lambda^2 - C_1} + \frac{B_2\lambda^2}{\lambda^2 - C_2} + \frac{B_3\lambda^2}{\lambda^2 - C_3}$ in Figure 2 provides the parameters $B_1 = 1.03051$, $C_1 = 4.92832 \ 10^{-3} \ \mu m^2$, $B_2 = 2.20788 \ 10^{-1}$, $C_2 = 3.002 \ 10^{-2} \ \mu m^2$, $B_3 = 1.00968$, and $C_3 = 1.03560 \ 10^2 \ \mu m^2$.

3. Apertures and Functional Optical Designs

In the following, we use the Prototype IP-Black photoresist to fabricate different optical devices, with the first being a 3D-printed pinhole camera. A sketch of the design is depicted in **Figure 3**a. The pinhole camera has a diameter of 760 µm and a height of 500 µm which demonstrates that the fabrication of high structures despite the absorption is possible. The pinhole itself has a radius of 12 µm and can be seen in Figure 3b. To improve the developing process, the structure has holes at the bottom providing better contact to the developer (visible in Figure 3c). The aperture on top is angled according to the beam path of the pinhole camera. In the image of a United States Air Force (USAF) test target, the test pattern is visible (Figure 3d), however, the imaging quality and contrast suffer from the low light level and from the partial transparency of the structure with thin parts, especially around the pinhole.

Since the black photoresist can be used for 3D direct laser writing, arbitrarily shaped apertures can easily be fabricated. In **Figure 4** apertures with a quadratic, as well as a circular outer boundary are depicted. We also demonstrate a combination of an aperture with the outer layer printed with the black photoresist forming a hollow cylinder and then filled it with silver metal ink NPS-J (NANOPASTE series, Harimatec, Inc.), which has a lower transmittance than the photoresist for better dimming.

To demonstrate contrast improvement by apertures we fabricate a hybrid design with a singlet lens made of IP-S and an aperture made of the Prototype IP-Black photoresist (**Figure 5**b,c). The IP-S lens with a diameter of 150 µm and height of 20 µm is fabricated with a laser power of 70% (pulse energy 508 pJ or intensity of 2.6 TW cm^{-2}), a scan speed of 50 mm/s, slicing 0.2 µm, and hatching 0.5 µm for good optical surface quality. The aperture has a circular shape with a height of 300 µm and a diameter of 650 µm. With these dimensions,
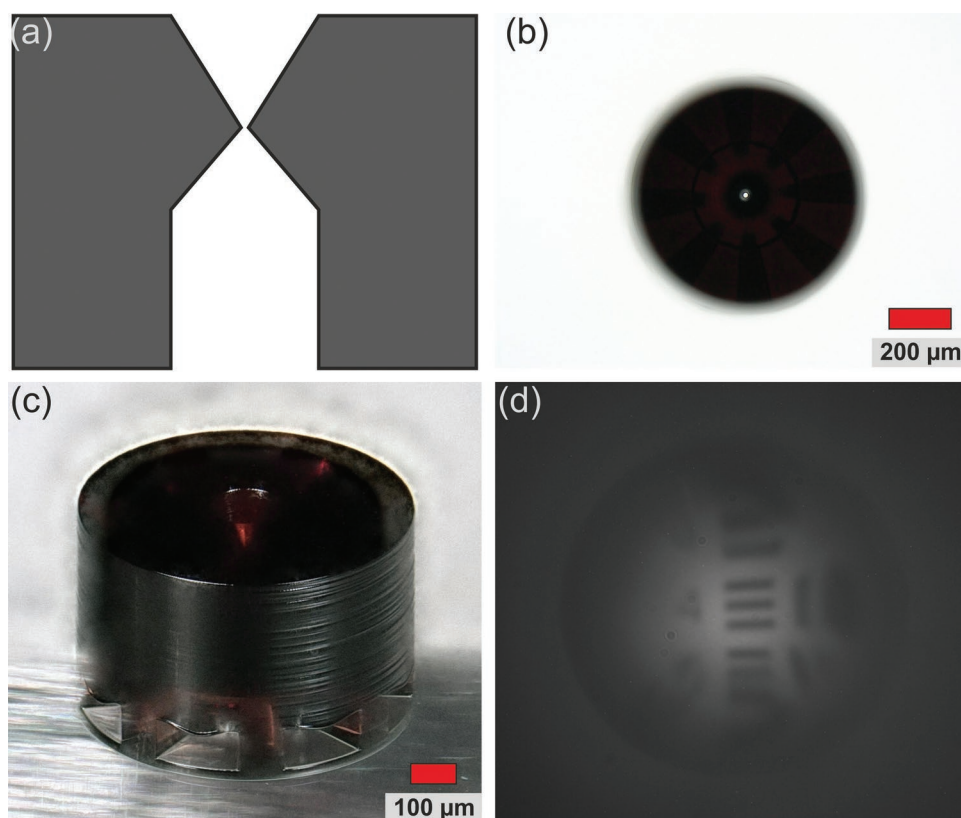

Figure 3. Pinhole camera printed with the black photoresist. a) Schematic cross-section of the pinhole camera, b) top view with through light illumination showing the absorbing structure around the pinhole and c) 60° angled view showing the hole design at the bottom of the structure for development. d) Pinhole imaging of a USAF target.
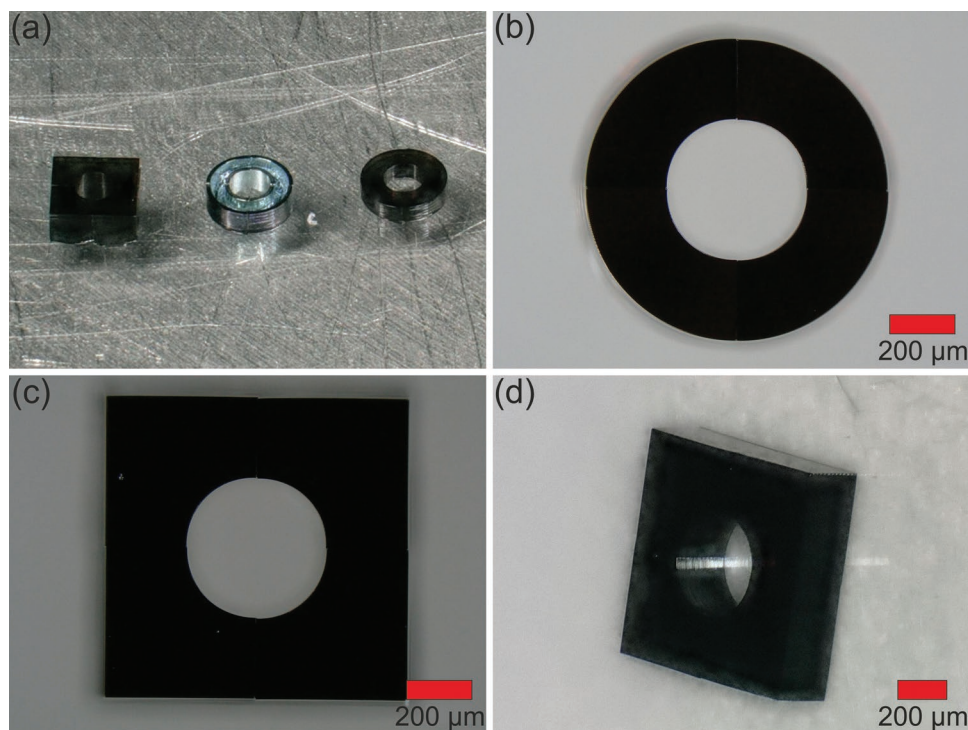
**ADVANCED
SCIENCE NEWS**

www.advancedsciencenews.com

**ADVANCED
FUNCTIONAL
MATERIALS**

www.afm-journal.de

Figure 4. Different apertures printed with the black photoresist. a) Overview with square, metal-filled, and round aperture. Close image of b) round and c) square apertures with d) an angled view.
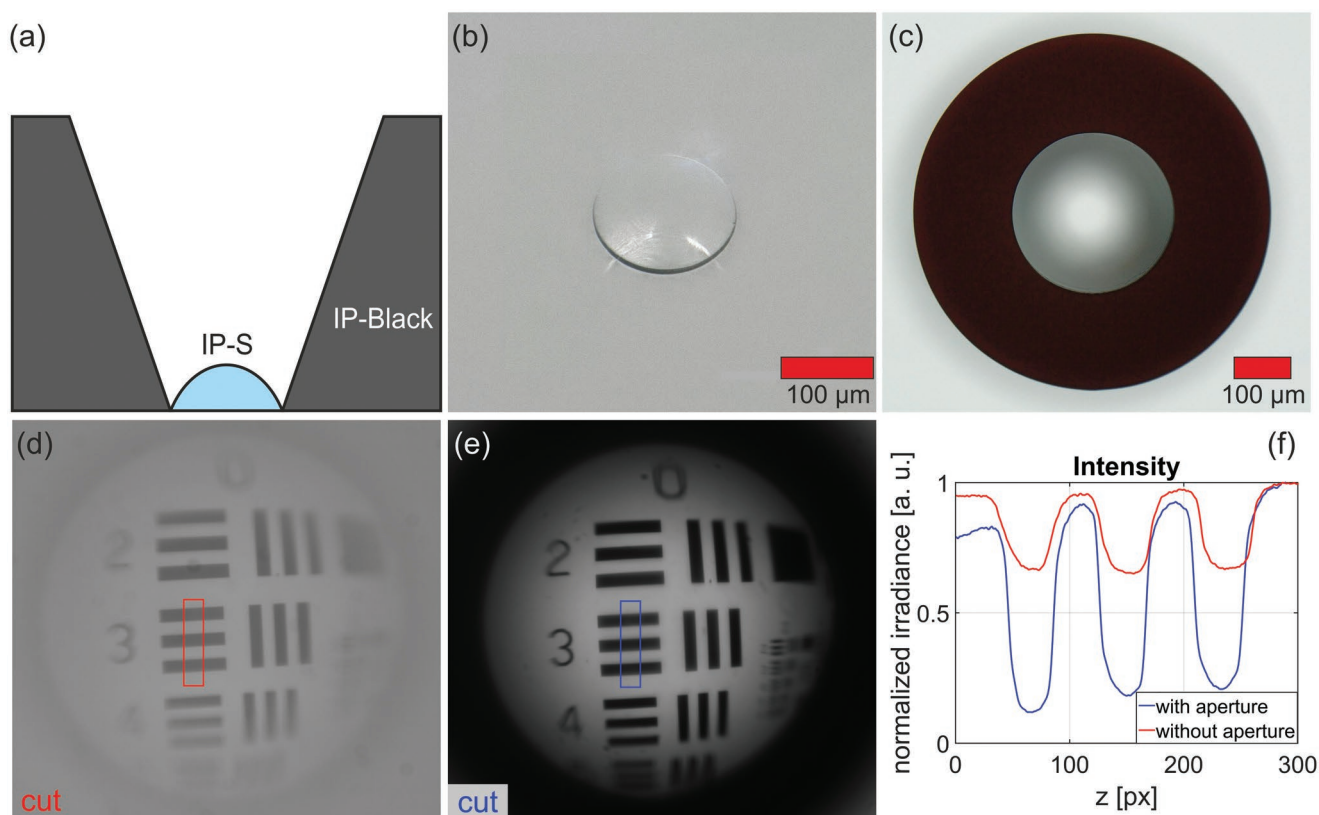

Figure 5. a) Hybrid lens design b) with IP-S singlet lens and c) Prototype IP-Black aperture. The imaging performance of the IP-S singlet d) without and e) with Prototype IP-Black aperture is shown. f) The red and blue rectangles in the images mark the area used for the contrast comparison, which nicely depicts the contrast improvement of more than a factor of four for the lens in combination with the aperture.
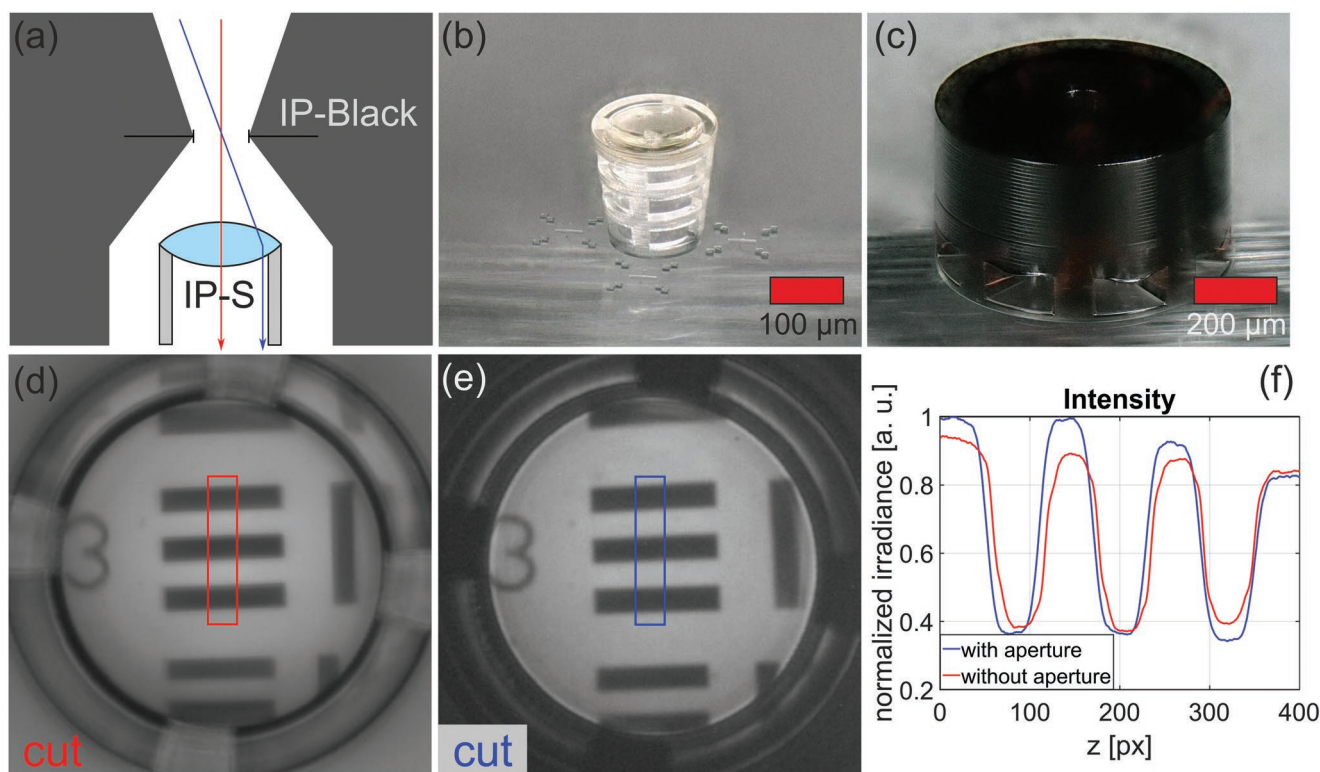
2211159 (4 of 8)

Figure 6. a) Hybrid telecentric design of b) IP-S lens and c) Prototype IP-Black aperture. Imaging performance of the telecentric design d) without and e) with Prototype IP-Black aperture. f) The red and blue rectangles in the images mark the area used for the contrast comparison.

we ensure high absorption of stray light. The opening angle is fitted to the NA of the micro-lens of 14°, leading to a diameter of 150 µm at the micro-lens and 300 µm at the top of the aperture. The design is depicted in Figure 5a. For the aperture made of the black photoresist, we use the same writing parameters as before. In the first step, the lens made of IP-S is printed and the aperture using the black photoresist is printed around it in the second step. For the multi-material printing, the sample has to be developed between the change of the photoresist (mr-Dev 600 for 15 min and afterward isopropanol for 5 min) and good alignment between the writing jobs is crucial. To ensure proper alignment, small markers are printed during the first job. The corresponding imaging result of a USAF test target is depicted in Figure 5d,e. It is clearly visible that the contrast in the image taken with the IP-S singlet exhibits a weak image contrast, which is drastically improved in combination with the 3D-printed aperture. A profile comparison of two intensity cuts through a line pair of the USAF test target for the singlet lens with and without a black aperture is depicted in Figure 5f showing an enhancement in the Michelson contrast defined by the equation $C_M = (I_{max} - I_{min})/(I_{max} + I_{min})$ of more than a factor of four.

More complex optical designs are possible with the black photoresist such as a telecentric lens design with an extended depth of focus depicted in **Figure 6**a, where the stop is situated in the front focal plane. In this design, a singlet lens made of IP-S is printed to the glass substrate using supporting leg structures that the distance to the glass substrate (image plane) and aperture is the focal distance (Figure 6b). In a second

fabrication step, a hull of the black photoresist is printed around the lens, forming the aperture placed in the focal plane of the lens (Figure 6c). The hull has an aperture diameter of 50 µm to maintain diffraction-limited performance across the full field of view of the telecentric lens. The total thickness (z) of the hull was chosen to be 500 µm to be well below the working distance of the 3D printing objective lens, yet thick enough for over 95% absorption in the bulk. The upper cone angles were designed to be just above the maximum field angles of the IP-S lens, i.e., 17° (design field of view +/–15°). Similar to the pinhole structure, our design of the Prototype IP-Black aperture comprises holes in the lower part for improved development of the photoresist. The contrast enhancement is not as prominent as in the singlet lens design depicted in the comparison of two intensity profiles of line pairs of a USAF test target (Figure 6d–f).

However, the lens with the additional stop offers more functionality, namely a longer depth of focus and telecentricity compared to a lens without an aperture. The extended depth of focus effect is demonstrated in **Figure 7**. Through-z scans of a USAF test target are recorded for a lens without (Figure 7a and with Figure 7b) the aperture and compared. Between each image, the target is moved 10 µm along the propagation axis for the lens without aperture and 30 µm for the telecentric lens with aperture. We find that the depth of focus of the telecentric design with aperture is about three times as long as the depth of focus of the reference lens without aperture, as expected for the improved case with aperture due to its reduced NA.

As demonstrated in the transmission measurements, the black photoresist with a height of 25 µm still transmits ≈75%
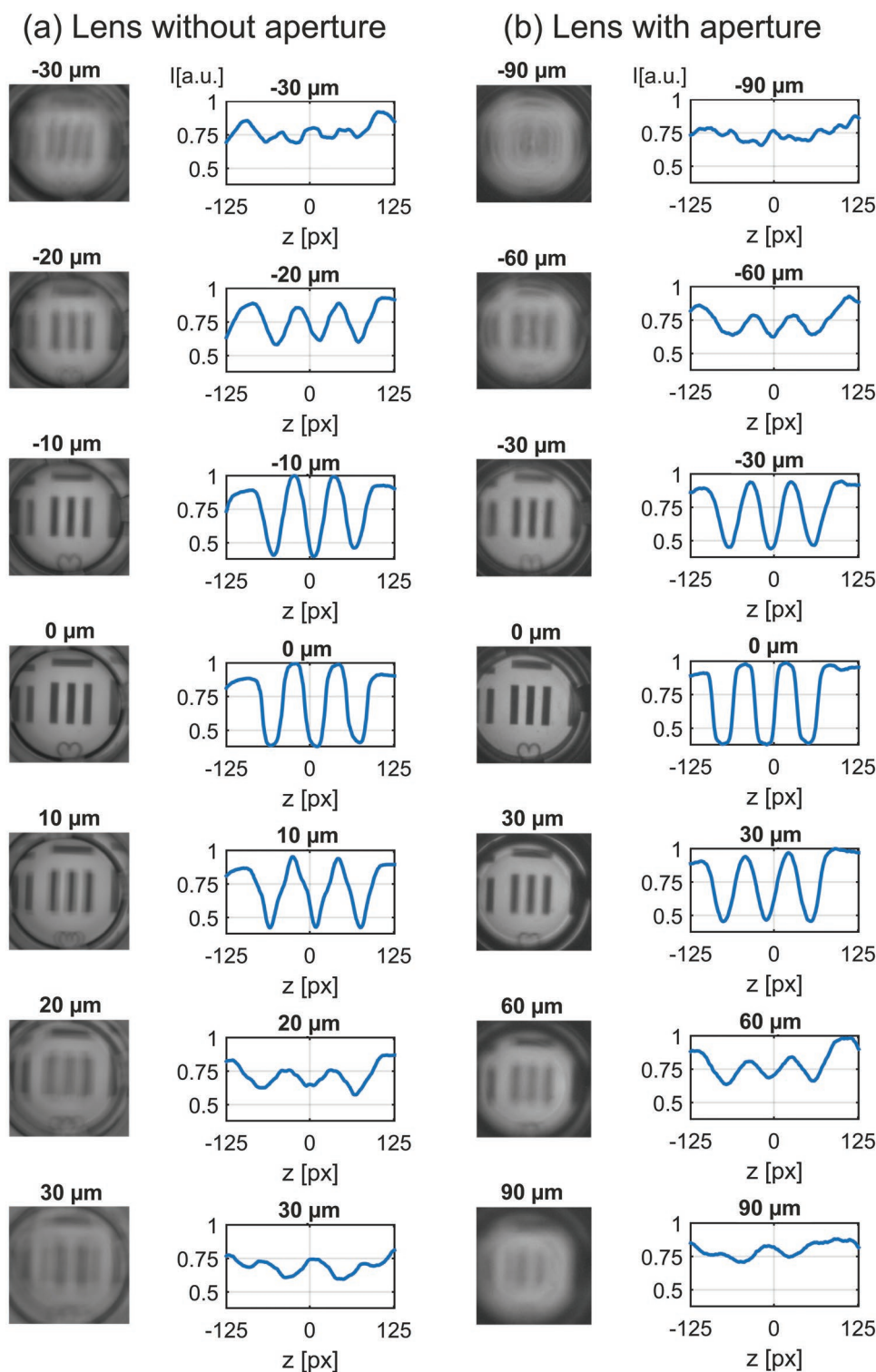
Figure 7. Through-z scans of imaging a USAF test target for a telecentric lens a) without and b) with Prototype IP-Black aperture. Each measurement series is normalized to the maximum in its focused image. The scan range is 60 µm for (a) and 180 µm for (b). Note that the depth of focus is about three times longer for the telecentric design with aperture due to the reduced NA.

of the incoming light intensity in the visible, thus it is possible to fabricate a thin singlet lens with the Prototype IP-Black photoresist and create the aperture directly in one single step. This reduces fabrication time and complexity drastically compared with multi-material designs. A singlet lens made of Prototype IP-Black without and with an aperture is
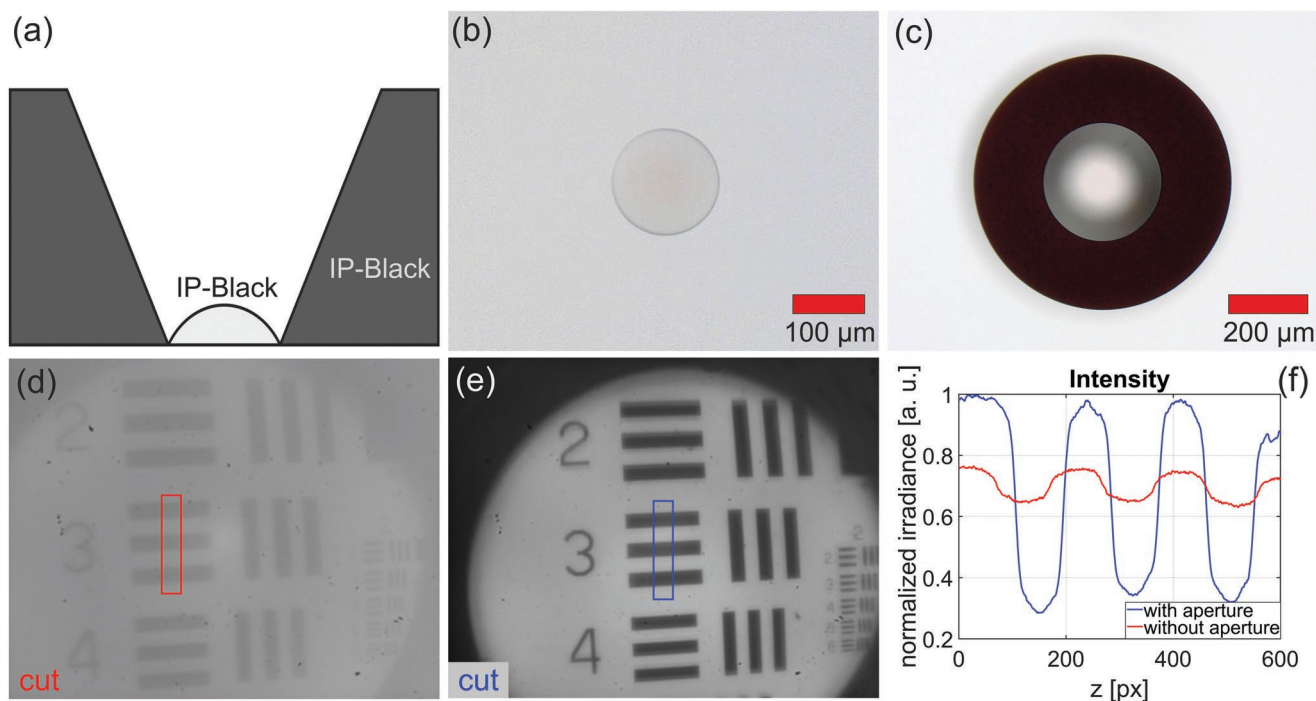
**ADVANCED
SCIENCE NEWS**

www.advancedsciencenews.com

**ADVANCED
FUNCTIONAL
MATERIALS**

www.afm-journal.de

Figure 8. a) The design for the Prototype IP-Black lens is identical to the singlet made of IP-S. 3D direct laser written one-step singlet lenses b) without and c) with aperture solely made of Prototype IP-Black. Imaging performance of the Prototype IP-Black singlet lens d) without and e) with aperture in one step. The red and blue rectangles in the images mark the area used for the contrast comparison. f) The contrast increases drastically by more than a factor of seven, as visible in the contrast comparison.

depicted in **Figure 8**b,c). The singlet lens is the same design as the IP-S singlet with a diameter of 150 µm and a height of 20 µm (Figure 8a). This is possible due to the fact that the dispersions of IP-S and Prototype IP-Black are almost identical. The writing parameters of Prototype IP-Black for the aperture are identical to those mentioned above. For the writing of the lens optical surface the writing parameters have to be adapted: Slicing 0.2 µm, hatching 0.5 µm. Furthermore, a hatching angle of 90 degrees between the layers exhibits the best surface results; printing the layers in parallel results in deformations. A hatching angle of 30 degrees results in the formation of a small spiral structure on top of the lenses. A longer piezo settling time of 2 s or even 5 s reduced these deformations. Figure 8 compares the imaging performance and contrast of the singlet Prototype IP-Black lens without (d) and with (e) an aperture. The contrast improves drastically in the image taken with the lens in combination with the aperture. Comparing the intensity cut through the image shows that the Michelson contrast improved by more than a factor of seven (see Figure 8f).

4. Conclusion

We introduced 3D direct laser writing of a black photoresist, which enables the fabrication of various new optical designs. Fabrication is possible due to the spectral transmission spectrum exhibiting high absorption in the visible but much lower absorption at the used fundamental laser wavelength of 780 nm. After characterizing important material parameters (absorption and dispersion) we demonstrated the use of the Prototype

IP-Black photoresist to fabricate a pinhole camera and show the possibility to create different apertures. While imaging contrast can be drastically improved by these apertures, the absorption at the aperture edges is limited. This imperfection, however, could also be used for targeted apodization design in future works. In the following section, we combined a Prototype IP-Black printed aperture in a two-step process with a lens made of transparent IP-S, improving the Michelson contrast by more than a factor of four. Due to the possibility of 3D printing, the black photoresist complex aperture geometries can be realized. We presented a telecentric design with an additional Prototype IP-Black aperture with a 3× increased depth of focus. Since the Prototype IP-Black photoresist still transmits more than 75% of the incoming light at a height of 20 µm (Figure 1b), we were able to create a singlet lens of the black photoresist in combination with an aperture in a one-step process, showing improved contrast compared to a reference lens without an aperture by more than a factor of seven. This approach enables faster fabrication and avoids alignment issues present in multi-material writing. These are just examples of possible designs with improved imaging quality. In general, the black photoresist offers a new one- and multi-material approach to further improve the performance of complex 3D printed micro-optics without the need for other fabrication methods used in the past, such as metal evaporation or the filling of printed cavities with metallic ink. Furthermore, it can be easily combined with other novel developments, such as anti-reflection atomic layer deposition coatings for reduced surface reflection[45] or newly introduced glass-based 2PP micro-optics offering improved stability and durability.[40]

Conflict of Interest

A patent has been filed concerning the fabrication of a lens and aperture both with the black photoresist in one fabrication step. Me and all coauthors except for Simon Mangold are involved in the patent.

Data Availability Statement

The data that support the findings of this study are available from the corresponding author upon reasonable request.

[1] V. Melissinaki, A. A. Gill, I. Ortega, M. Vamvakaki, A. Ranella, J. W. Haycock, C. Fotakis, M. Farsari, F. Claeyssens, *Biofabrication* **2011**, *3*, 045005.

[2] H. Eto, H. G. Franquelim, M. Heymann, P. Schwille, *Soft Matter* **2021**, *17*, 5456.

[3] A. Selimis, V. Mironov, M. Farsari, *Microelectron. Eng.* **2015**, *132*, 83.

[4] G. Weisgrab, A. Ovsianikov, P. F. Costa, *Adv. Mater. Technol.* **2019**, *4*, 1900275.

[5] Y. Liao, Y. Cheng, C. Liu, J. Song, F. He, Y. Shen, D. Chen, Z. Xu, Z. Fan, X. Wei, K. Sugioka, K. Midorikawa, *Lab Chip* **2013**, *13*, 1626.

[6] R. Acevedo, Z. Wen, I. B. Rosenthal, E. Z. Freeman, M. Restaino, N. Gonzalez, R. D. Sochol, in *Proceedings of the IEEE International Conf. on Micro Electro Mechanical Systems (MEMS)*, Institute of Electrical, Gainesville **2021**, 10.

[7] R. K. Jayne, M. Ç. Karakan, K. Zhang, N. Pierce, C. Michas, D. J. Bishop, C. S. Chen, K. L. Ekinci, A. E. White, *Lab Chip* **2021**, *21*, 1724.

[8] J. Knoška, L. Adriano, S. Awel, K. R. Beyerlein, O. Yefanov, D. Oberthuer, G. E. Peña Murillo, N. Roth, I. Sarrou, P. Villanueva-Perez, M. O. Wiedorn, F. Wilde, S. Bajt, H. N. Chapman, M. Heymann, *Nat. Commun.* **2020**, *11*, 657.

[9] S. Thiele, K. Arzenbacher, T. Gissibl, H. Giessen, A. M. Herkommer, *Sci. Adv.* **2017**, *3*, e1602655.

[10] S. Ristok, S. Thiele, A. Toulouse, A. M. Herkommer, H. Giessen, *Opt. Mater. Express* **2020**, *10*, 2370.

[11] P. I. Dietrich, M. Blaicher, I. Reuter, M. Billah, T. Hoose, A. Hofmann, C. Caer, R. Dangel, B. Offrein, U. Troppenz, M. Moehrle, W. Freude, C. Koos, *Nat. Photonics* **2018**, *12*, 241.

[12] A. Landowski, D. Zepp, S. Wingerter, G. Von Freymann, A. Widera, *APL Photonics* **2017**, *2*, 106102.

[13] A. Bertoncini, C. Liberale, C. Liberale, *Opt* **2020**, *7*, 1487.

[14] S. Thiele, T. Gissibl, H. Giessen, A. M. Herkommer, *Opt. Lett.* **2016**, *41*, 3029.

[15] S. Schmidt, S. Thiele, A. Toulouse, C. Bösel, T. Tiess, A. Herkommer, H. Gross, H. Giessen, *Optica* **2020**, *7*, 1279.

[16] B. Chen, D. Claus, D. Russ, M. R. Nizami, *Opt. Lett.* **2020**, *45*, 5583.

[17] S. Varapnickas, S. Chandran Thodika, F. Moroté, S. Juodkazis, M. Malinauskas, E. Brasselet, *Appl. Phys. Lett.* **2021**, *118*, 151104.

[18] A. Toulouse, J. Drozella, S. Thiele, H. Giessen, A. Herkommer, A. Toulouse, J. Drozella, S. Thiele, H. Giessen, A. Herkommer, *Light Adv. Manuf.* **2021**, *2*, 20.

[19] D. Zhang, H. Wei, H. Hu, S. Krishnaswamy, *APL Photonics* **2020**, *5*, 076112.

[20] D. Zhang, Z. Zhang, H. Wei, J. Qiu, S. Krishnaswamy, *Photonics Res.* **2021**, *9*, 1984.

[21] K. Prause, S. Thiele, A. M. Herkommer, H. Giessen, B. Pinzer, M. Layh, *Opt. Eng.* **2020**, *59*, 035102.

[22] P. Dietrich, G. Göring, M. Trappen, M. Blaicher, W. Freude, T. Schimmel, H. Hölscher, C. Koos, *Small* **2020**, *16*, 1904695.

[23] A. J. Thompson, M. Power, G.-Z. Yang, *Opt. Express* **2018**, *26*, 14186.

[24] S. Rekštyte, D. Paipulas, M. Malinauskas, V. Mizeikis, *Nanotechnology* **2017**, *28*, 124001.

[25] V. Melissinaki, O. Tsilipakos, M. Kafesaki, M. Farsari, S. Pissadakis, *IEEE J. Sel. Top. Quantum Electron.* **2021**, *27*, 1.

[26] C. Liberale, P. Minzioni, F. Bragheri, F. De Angelis, E. Di Fabrizio, I. Cristiani, *Nat. Photonics* **2007**, *1*, 723.

[27] A. Asadollahbaik, S. Thiele, K. Weber, A. Kumar, J. Drozella, F. Sterl, A. M. Herkommer, H. Giessen, J. Fick, *ACS Photonics* **2020**, *7*, 88.

[28] J. Li, S. Thiele, B. C. Quirk, R. W. Kirk, J. W. Verjans, E. Akers, C. A. Bursill, S. J. Nicholls, A. M. Herkommer, H. Giessen, R. A. McLaughlin, *Light Sci. Appl.* **2020**, *9*, 124.

[29] J. Li, P. Fejes, D. Lorenser, B. C. Quirk, P. B. Noble, R. W. Kirk, A. Orth, F. M. Wood, B. C. Gibson, D. D. Sampson, R. A. McLaughlin, *Sci. Rep.* **2018**, *8*, 14789.

[30] F. Akhoundi, Y. Qin, N. Peyghambarian, J. K. Barton, K. Kieu, *Biomed. Opt. Express* **2018**, *9*, 2326.

[31] C. J. Sheil, U. Khan, Y. N. Zakharov, M. F. Coughlan, D. K. Pleskow, M. S. Sawhney, T. M. Berzin, J. M. Cohen, M. Glyavina, L. Zhang, I. Itzkan, L. T. Perelman, L. Qiu, *Opt. Lasers Eng.* **2021**, *142*, 106616.

[32] K. Weber, Z. Wang, S. Thiele, A. Herkommer, H. Giessen, *Opt. Lett.* **2020**, *45*, 2784.

[33] T. Gissibl, S. Thiele, A. Herkommer, H. Giessen, *Nat. Photonics* **2016**, *10*, 554.

[34] D. Gailevičius, V. Padolskytė, L. Mikoliūnaitė, S. Šakirzanovas, S. Juodkazis, M. Malinauskas, *Nanoscale Horiz.* **2019**, *4*, 647.

[35] A. Toulouse, J. Drozella, P. Motzfeld, N. Fahrbach, V. Aslani, S. Thiele, H. Giessen, A. Herkommer, *Opt. Express* **2022**, *30*, 707.

[36] S. Thiele, C. Pruss, A. M. Herkommer, H. Giessen, *Opt. Express* **2019**, *27*, 35621.

[37] M. Schmid, S. Thiele, A. Herkommer, H. Giessen, *Opt. Lett.* **2018**, *43*, 5837.

[38] M. Schmid, F. Sterl, S. Thiele, A. Herkommer, H. Giessen, *Opt. Lett.* **2021**, *46*, 2485.

[39] F. Rothermel, S. Thiele, C. Jung, H. Giessen, A. Herkommer, *Optomechanics and Optical Alignment* **2021**, *11816*, 134.

[40] D. Gonzalez-Hernandez, S. Varapnickas, G. Merkininkaitė, A. Čiburys, D. Gailevičius, S. Šakirzanovas, S. Juodkazis, M. Malinauskas, *Photonics 2021* **2021**, *8*, 577.

[41] G. Merkininkaitė, E. Aleksandravičius, M. Malinauskas, D. Gailevičius, S. Šakirzanovas, *Opto-Electronic Adv* **2022**, *5*, 210077.

[42] A. Toulouse, S. Thiele, H. Giessen, A. M. Herkommer, *Opt. Lett.* **2018**, *43*, 5283.

[43] A. Toulouse, S. Thiele, K. Hirzel, M. Schmid, K. Weber, M. Zyrianova, H. Giessen, A. M. Herkommer, M. Heymann, *Opt. Mater. Express* **2022**, *12*, 3801.

[44] M. Schmid, D. Ludescher, H. Giessen, *Opt. Mater. Express* **2019**, *9*, 4564.

[45] S. Ristok, P. Flad, H. Giessen, *Opt. Mater. Express* **2022**, *12*, 2063.